

Isotropic and Anisotropic Hyperfine Interactions in Hydrazyl and Carbazyl

N. W. Lord and S. M. Blinder

Citation: *The Journal of Chemical Physics* **34**, 1693 (1961); doi: 10.1063/1.1701066

View online: <http://dx.doi.org/10.1063/1.1701066>

View Table of Contents: <http://scitation.aip.org/content/aip/journal/jcp/34/5?ver=pdfcov>

Published by the AIP Publishing

Articles you may be interested in

[Paramagnetism of Carbazyl and Hydrazyl Free Radicals](#)

J. Chem. Phys. **46**, 456 (1967); 10.1063/1.1840688

[Isotropic Proton Hyperfine Interaction and Properties of the CH Bond](#)

J. Chem. Phys. **39**, 3455 (1963); 10.1063/1.1734214

[Proton Hyperfine Spectra of Diphenyl Picryl Hydrazyl](#)

J. Chem. Phys. **32**, 1584 (1960); 10.1063/1.1730977

[Isotropic Proton Hyperfine Interaction in the Methyl Radical](#)

J. Chem. Phys. **32**, 52 (1960); 10.1063/1.1700946

[Isotropic Hyperfine Interactions in Aromatic Free Radicals](#)

J. Chem. Phys. **25**, 890 (1956); 10.1063/1.1743137



Isotropic and Anisotropic Hyperfine Interactions in Hydrazyl and Carbazyl*

N. W. LORD† AND S. M. BLINDER

Applied Physics Laboratory, The Johns Hopkins University, Silver Spring, Maryland

(Received October 12, 1960)

This paper describes a detailed experimental and theoretical study of the hyperfine structure of diphenylpicrylhydrazyl (hydrazyl) and picrylaminocarbazyl (carbazyl). Both isotropic and anisotropic hyperfine interactions involving the α and β nitrogen atoms are considered. Experimentally, electron spin resonance spectra are observed for dilute solutions of each radical in both fluid and solid media. Concentrations of the order of 0.001 M are employed so as to minimize dipolar and exchange interactions among radicals. The fluid spectra yield, in straightforward fashion, the absolute values of the isotropic coupling constants $|A_1|$ and $|A_2|$. These splitting parameters are chosen such that a synthesized line shape composed of Gaussians gives optimal reproduction of the observed resonance profile. For the solid solutions, Duco cement (with hydrazyl) and Lucite (with carbazyl) provide glassy trapping matrices. It is assumed that the radicals are frozen in an ensemble of random orientations in these solids. Appropriate theoretical line shapes, considering interactions with two magnetic nuclei, are derived, and values

assigned to the anisotropic parameters B_1 and B_2 from comparison of experimental and theoretical resonance patterns. The isotropic constants are assumed to be unchanged in the transition from liquid to solid solution. It is found moreover that the inherent Gaussian half-width σ is approximately the same in both states. The parameters assigned through our analysis are Hydrazyl— $A_1=9.35\pm 0.20$ gauss; $A_2=7.85\pm 0.20$ gauss; $B_1=6.6\pm 0.5$ gauss; $B_2=5.8\pm 0.5$ gauss; $\sigma=3.36\pm 0.20$ gauss. Carbazyl— $A_1=10.2\pm 0.5$ gauss; $A_2=5.8\pm 0.5$ gauss; $B_1=7.7\pm 1.0$ gauss; $B_2=4.1\pm 1.0$ gauss; $\sigma=3.4\pm 0.5$ gauss. Resonance of the hydrazyl-Duco solution during incipient solidification was also observed. In this intermediate medium the anisotropic hyperfine interactions are only partially averaged out by molecular motions. It was found possible to characterize the rigidity of the medium by a parameter λ ($0\leq\lambda\leq 1$) such that each anisotropic parameter is exhibited in the spectrum as if it were λ times its full value. Various implications of our results on the structure of hydrazyl and carbazyl are considered. One conclusion drawn is that both radicals are largely planar in configuration.

I. INTRODUCTION

THE parameters which characterize the hyperfine coupling in a free radical are of considerable chemical interest since these relate to the distribution of the change and spin in the radical. These parameters may be assigned from detailed analysis of the orientation-dependent electron spin resonance (ESR) spectrum of a single crystal containing the radical. Some very thorough studies along these lines have recently been reported by three groups of workers.¹ In single-crystal studies, however, some rather formidable difficulties are often encountered. These may include preparation of the crystalline sample and its crystallographic characterization as well as analysis and interpretation of complex spectra, particularly when there is more than one molecular orientation corresponding to one crystal orientation.

We propose and illustrate in this paper an alternative to single crystal analysis. Our method is capable of yielding almost as much useful information while requiring somewhat less experimental work. The only condition for its applicability is that it be possible to observe ESR spectra of a free radical dispersed in both fluid and solid media. This holding, at least two of the three hyperfine coupling parameters can be assigned.

Our procedure should be applicable to a large class of stable polyatomic free radicals.²

The basis of the method is the following. The hyperfine coupling consists of two parts: an isotropic part (A term) containing a single scalar parameter A , and an anisotropic part (B term) characterized by any two of the principal values of the traceless tensor \mathcal{B} . In fluid medium, where the molecules are subjected to high-frequency reorientations, the tensor term is effectively averaged to zero.³ In the solid, however, the B term combines with the A term to produce orientation-dependent ESR spectra.⁴ In single crystals the resonances generally remain sharp but their frequencies become dependent on the orientation of the molecule with respect to the magnetic field. In polycrystalline media, a superposition of single-crystal resonances results and broad, widely spaced ESR lines are observed. From the positions of the peaks in the latter (and secondarily from the line shape) a second hyperfine coupling parameter may be determined. In cases of local cylindrical symmetry (*vide infra*), two parameters suffice to characterize the hyperfine interaction

² Extension to include unstable radicals might also be possible. This could be accomplished by observation of (a) the fluid ESR spectrum by the new steady-state technique [L. H. Piette and W. C. Landgraf, *J. Chem. Phys.* **32**, 1107 (1960)] and (b) the spectrum of the free radical trapped in an inert matrix [C. K. Jen, S. N. Foner, E. L. Cochran, and V. A. Bowers, *Phys. Rev.* **112**, 1169 (1958)].

³ S. I. Weissman, *J. Chem. Phys.* **22**, 1378 (1954).

⁴ We presume that the molecule is not free to rotate (or tunnel with high frequency) in the solid. Small radicals, e.g., NH_2 , CH_3 , may exhibit such behavior. See H. M. McConnell, *J. Chem. Phys.* **29**, 1422 (1958); C. K. Jen in *Formation and Trapping of Free Radicals*, edited by A. M. Bass and H. P. Broida (Academic Press, Inc., New York, 1960), pp. 237–238.

* Work supported by Bureau of Naval Weapons, Department of the Navy.

† Present address: Hudson Laboratories, Columbia University, Dobbs Ferry, New York.

¹ D. K. Ghosh and D. H. Whiffen, *Mol. Phys.* **2**, 285 (1959); I. Miyagawa and W. Gordy, *J. Chem. Phys.* **30**, 1590 (1959); **32**, 255 (1960); H. M. McConnell, C. Heller, T. Cole, and R. W. Fessenden, *J. Am. Chem. Soc.* **82**, 766 (1960); C. Heller and H. M. McConnell, *J. Chem. Phys.* **32**, 1535 (1960).

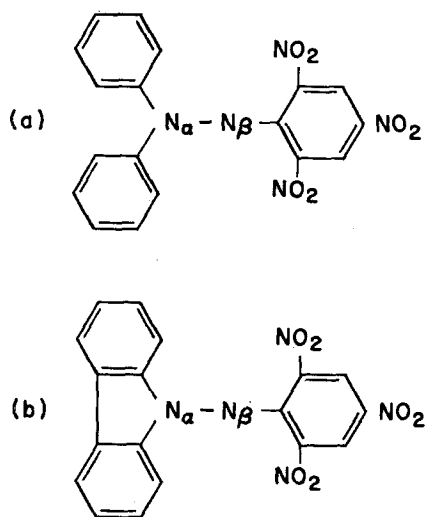


FIG. 1. Structural formulas; (a) hydrazyl, (b) carbazyl. The central nitrogen atoms are labeled by the subscripts α and β .

completely. These may unambiguously be assigned (except perhaps for sign) from correlation of the fluid and solid spectra. It is necessary that the free radicals be dispersed in a diamagnetic matrix in order to minimize dipolar and exchange interactions.

In this paper we shall apply our method to two stable organic free radicals, α , α -diphenyl- β -picrylhydrazyl (DPPH), hereafter referred to as hydrazyl, and N -picryl-9-aminocarbazyl, hereafter referred to as carbazyl (see Fig. 1).

II. GENERAL THEORY

The theoretical basis underlying this paper has been given in detail by one of the authors.⁵ To be applicable to the present work, these results must be extended to the case of two magnetic nuclei interacting with an electron spin. The necessary generalization is outlined in this section.

We begin with the spin Hamiltonian for Zeeman and magnetic hyperfine interactions involving one unpaired electron and one magnetic nucleus

$$\mathcal{H}(\mathbf{S}, \mathbf{I}) = -g\mu_0\mathbf{H}\cdot\mathbf{S} + A\mathbf{S}\cdot\mathbf{I} + \mathbf{S}\cdot\mathcal{B}'\cdot\mathbf{I}, \quad (1)$$

with

$$A\mathbf{S} = -gg_I\mu_0\mu_N(8\pi/3)\langle\sum_k\delta(\mathbf{r}_k)\mathbf{S}_k\rangle \quad (2)$$

and

$$\mathcal{B}' = -gg_I\mu_0\mu_N\langle 3\mathbf{r}\mathbf{r}\mathbf{r} - \mathfrak{J}r^{-3}\rangle. \quad (3)$$

Here \mathbf{r}_k is the position vector of electron k in a space-fixed coordinate system with origin at the magnetic nucleus. The three parts of (1) represent, respectively, the electron Zeeman energy, the isotropic hyperfine interaction, and the tensor hyperfine coupling. In a large magnetic field the first term is the dominant contribution to the magnetic energy of the system. We shall

neglect the analogous nuclear Zeeman term.^{5a} Implicit in the Hamiltonian (1) is the assumption that the electron magnetic moment is due entirely to spin. In the polyatomic free radicals under consideration in this paper, orbital momenta are almost totally "quenched" by asymmetric molecular or crystal fields. Consequently, the anisotropy in the g tensor should be rather small. We shall assume that g is effectively a scalar with value very close to that of the free electron. Experimental evidence bearing on this point will be discussed in Sec. III. Such additional complications as quadrupole coupling and spin-rotational interactions will not be considered. The expectation value brackets in (2) and (3) denote averages over the complete molecular wave function. In the B part (3), the bracket is effectively an integral over the orbital of the unpaired electron. The A term (2), however, will, in general, include contributions from other orbitals as a consequence of spin polarization (see Sec. IX).

Following footnote 5, the tensor \mathcal{B}' is transformed to its molecule-fixed principal axis system by an orthogonal transformation involving the Eulerian angles

$$\mathcal{B}' = Q^{-1}(\theta, \phi, \chi)\mathcal{B}Q(\theta, \phi, \chi). \quad (4)$$

The principal values of \mathcal{B} are then the diagonal elements of its matrix representation

$$\mathcal{B} = \begin{bmatrix} B_{xx} & 0 & 0 \\ 0 & B_{yy} & 0 \\ 0 & 0 & B_{zz} \end{bmatrix}, \quad (5)$$

where

$$B_{xx} + B_{yy} + B_{zz} = 0. \quad (6)$$

The angular coordinates are defined as shown in Fig. 2.

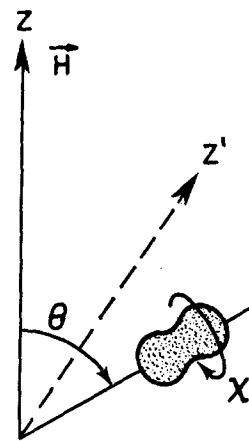


FIG. 2. Coordinate system for spin Hamiltonian. Z is the direction of the static magnetic field, z is the figure axis of the molecule, and Z' , the direction of the electron spin's magnetic field at the nucleus. θ , ϕ , χ are the Eulerian angles connecting the molecule-fixed xyz axes with the space-fixed XYZ axes.

^{5a} A N^{14} nucleus at X -band frequency (3300-gauss field) has a maximum Zeeman energy corresponding to 0.36 gauss. This may be neglected for our purposes. For protons, however, this quantity is 2.5 gauss and may no longer be negligible. In particular, satellite lines may result under such circumstances. See G. T. Trammell, H. Zeldes, and R. Livingston, *Phys. Rev.* **110**, 630 (1958).

⁵ S. M. Blinder, *J. Chem. Phys.* **33**, 748 (1960).

The hyperfine coupling of a nucleus is characterized by three parameters: A , and two of the principal values of \mathcal{B} . It is convenient for what follows to define two auxiliary parameters

$$\left. \begin{aligned} B &\equiv \frac{1}{2}B_{zz} = -\frac{1}{2}(B_{xx} + B_{yy}) \\ C &\equiv \frac{1}{2}(B_{xx} - B_{yy}) \end{aligned} \right\} \quad (7)$$

In terms of the molecular wave function, these are given by

$$\left. \begin{aligned} B &= -\frac{1}{2}gg_I\mu_0\mu_N \langle (3z^2 - r^2)/r^5 \rangle \\ C &= -\frac{3}{2}gg_I\mu_0\mu_N \langle (x^2 - y^2)/r^5 \rangle \end{aligned} \right\} \quad (8)$$

With the odd-electron charge distribution about a nucleus has at least a threefold axis of symmetry, in particular, for cylindrical symmetry, two of the principal values of \mathcal{B} become degenerate. Choosing z as the symmetry axis, C vanishes and the hyperfine interaction is now characterized by just two constants, A and B ; C is evidently a measure of deviation from axial symmetry. The hyperfine coupling with some particular magnetic nucleus exhibits cylindrical symmetry if the singly occupied orbital partakes only of s and p character with reference to that nucleus. Significant admixture of higher-orbital character, for example, d or f , would, of course, introduce nonaxial contributions. If there are more than one hyperfine-coupled nuclei in the molecule, there can no longer be rigorous cylindrical symmetry about any one. However, should the unpaired electron's orbital still contain principally s and p character about some nucleus, we would ascribe to that nucleus "local cylindrical symmetry." In most cases, we might expect the deviation from rigorous cylindrical symmetry to be quite small whenever local cylindrical symmetry prevails. It is important to note that for a prolate charge distribution, $B > 0$. This too will obtain whenever the orbital contains predominantly s and p character. As we shall subsequently show, hydrazyl and carbazyl exhibit, to good approximation, local cylindrical symmetry about both central nitrogen nuclei. Hence, we shall be particularly concerned with results pertaining to this special case.

We wish now to compute the orientation-dependent eigenvalues of the spin Hamiltonian. This is most conveniently approached by perturbation theory, the electronic Zeeman coupling serving as the unperturbed Hamiltonian, the hyperfine terms as perturbation operators. Carrying the perturbation expansion to first order we obtain

$$E(M_S, M_I') = -g\mu_0 H M_S + K(\theta, \chi) M_S M_I', \quad (9)$$

where

$$\begin{aligned} K^2 &= A^2 + 2AB(3 \cos^2\theta - 1) + B^2(3 \cos^2\theta + 1) \\ &+ C^2 \sin^2\theta + 2C(A - B) \sin^2\theta(\cos^2\chi - \sin^2\chi). \end{aligned} \quad (10)$$

Physically speaking, the electron spin is coupled strongly to the external field \mathbf{H} . Thus only the Z component of \mathbf{S} is stationary. Presuming, as before, that hyperfine terms are much larger than nuclear Zeeman terms, the nuclear spin is most strongly coupled to the electron's tensor field. Consequently, the two spins have, in general, different axes of quantization. The first-order perturbation treatment turns out to be equivalent to finding an effective axis of quantization for the nuclear spin. This axis, denoted by Z' in Fig. 2, represents the direction of the electron spin's magnetic field at the nucleus. M_I' in Eq. (9) is then the quantized component of \mathbf{I} along Z' .

If the odd-electron charge density has axial symmetry in the locality of the magnetic nucleus, then $C = 0$ and the lower line of the expression for K [Eq. (10)] vanishes. All dependence on the angle χ is thereby removed to accuracy of first order. It is not necessary for our purposes to carry the perturbation expansion beyond first order. For X -band spectroscopy, transitions arising from second-order mechanisms are of considerably reduced intensity.⁶

In first order, the selection rules for ESR transitions are $\Delta M_S = \pm 1$, $\Delta M_I' = 0$. The observed hyperfine frequency shifts for cylindrical symmetry are given by

$$\nu = [A^2 + 2AB(3 \cos^2\theta - 1) + B^2(3 \cos^2\theta + 1)]^{1/2} M_I'. \quad (11)$$

When $|A| \gg |B|$, the root may be expanded to yield the familiar $(3 \cos^2\theta - 1)$ -angular dependence. Equation (11) applies to an oriented single crystal. In a polycrystalline sample we would observe the ensemble distribution of single crystal resonances. The range of resonance absorption is then bracketed by the frequencies $|A - B| M_I'$ and $|A + 2B| M_I'$.

We denote the theoretical shape of the powder spectrum by $g(\nu)$. This is a sum of $2I + 1$ component line-shape functions, one for each M_I' ,

$$g(\nu) = \sum_{M=-I}^I g_M(\nu). \quad (12)$$

If each component is normalized to unity [with $g_0(\nu) = \delta(\nu)$], $g(\nu)$ is normalized to $2I + 1$. The fraction of molecules (or crystallites) having polar angle between θ and $\theta + d\theta$ is $\frac{1}{2} \sin\theta d\theta$. The corresponding resonance frequencies are denoted by ν and $\nu + d\nu$. We have thus

$$g_M(\nu) d\nu = \frac{1}{2} \sin\theta d\theta, \quad (13)$$

ν being implicitly dependent on θ through (11). Consequently,

$$g_M(\nu) = -\frac{1}{2}(d \cos\theta)/d\nu = -\frac{1}{2}[d\nu/(d \cos\theta)]^{-1}. \quad (14)$$

For convenience, we may label the high-frequency ($\nu > 0$) part of the spectrum with $M > 0$, the low-

⁶ In higher frequency ranges, say the K band, second-order transitions may become important. See I. Miyagawa and W. Gordy, *J. Chem. Phys.* **32**, 255 (1960).

frequency part ($\nu < 0$) with $M < 0$. Accordingly, a normalized hyperfine component line shape is given by

$$g_M(\nu) = \frac{\nu(\theta)}{(6AB + 3B^2)M^2 \cos\theta} \quad (15)$$

It is necessary now to derive a corresponding expression for two magnetic nuclei. In general, the \mathcal{B} tensor will have a different set of principal axes about each nucleus, depending upon the local electron spin distribution. Consequently, the angular specification of molecular orientation will be different for each nucleus. The dependence of the composite hyperfine structure on the orientation of the molecule will be thus a rather complicated function of the various θ 's and χ 's. The composite line shape does, however, assume a simple form if for both nuclei there is cylindrical symmetry with the two z axes parallel. Then the same angle θ pertains to either nucleus and may be ascribed to the molecule as a whole. Composite hyperfine frequency shifts are sums (or differences) of those for the individual nuclei, i.e.,

$$\nu_{M_1 M_2} = \nu_{M_1 0} + \nu_{0 M_2}. \quad (16)$$

Denoting by $g_{M_1 0}(\nu)$ and $g_{0 M_2}(\nu)$ the powder line shape associated with nucleus 1 and 2, we may write, analogous to (14)

$$\left. \begin{aligned} \frac{1}{g_{M_1 0}(\nu)} &= -2 \frac{d\nu_{M_1 0}}{d \cos\theta_1} \\ \frac{1}{g_{0 M_2}(\nu)} &= -2 \frac{d\nu_{0 M_2}}{d \cos\theta_2} \end{aligned} \right\} \quad (17)$$

Also,

$$\frac{1}{g_{M_1 M_2}(\nu)} = -2 \frac{d\nu_{M_1 M_2}}{d \cos\theta} \quad (18)$$

where $g_{M_1 M_2}(\nu)$ is the composite line shape. Since $\theta_1 = \theta_2 = \theta$, it follows that

$$\frac{1}{g_{M_1 M_2}(\nu)} = \frac{1}{g_{M_1 0}(\nu)} + \frac{1}{g_{0 M_2}(\nu)}, \quad (19)$$

the equality holding for each value of θ . The $g_{M_1 M_2}(\nu)$ is suitably normalized to unity. The over-all composite line shape is then

$$g(\nu) = \sum_{M_1=-I_1}^{I_1} \sum_{M_2=-I_2}^{I_2} g_{M_1 M_2}(\nu) \quad (20)$$

and is normalized to $(2I_1 + 1)(2I_2 + 1)$.

In discussing line shape we have, thus far, neglected the influence of other factors. The latter might include dipolar broadening, exchange interaction, anisotropy in g , unresolved hyperfine structure associated with other magnetic nuclei, as well as various factors inherent in the experimental procedure, e.g., field homogeneity, power saturation, and field modulation. Additional

broadening of the two-nucleus line shape would also occur should there be any deviation from parallelism of the principal axis systems. The line shape from all factors excluding hyperfine angular dependence may generally be represented by either a Gaussian or a Lorentzian distribution function. The observed line shape might then be approximated by an integral transformation of $g(\nu)$

$$g_{\text{exp}}(\nu) = \int d\nu' g(\nu') G(\nu - \nu'), \quad (21)$$

where the kernel $G(\nu - \nu')$ specifies the inherent broadening. In this paper we shall use Gaussians for the $G(\nu - \nu')$ with parameters inferred from the corresponding spectra in fluid media.

Usually it is the derivative of $g_{\text{exp}}(\nu)$ which is observed directly. Since the functions $g_M(\nu)$ are discontinuous at the frequencies $|A - B|M$ and $|A + 2B|M$, we might expect maxima and minima in $g_{\text{exp}}'(\nu)$ to occur close to these frequencies (and the corresponding ones for the composite lines). These provide important clues in the assignment of the B parameters from the solid spectra.

III. HYDRAZYL AND CARBAZYL

Several tri-aryl-substituted hydrazyl free radicals have been found to be stable at room temperature. The most extensively studied of these, diphenylpicrylhydrazyl, was first prepared in 1922.⁷ During the past ten years, the technique of electron spin resonance has stimulated renewed interest in this class of free radicals.

Resonance absorption by crystalline hydrazyl was first reported by Holden, *et al.*,⁸ and by Townes and Turkevich.⁹ The sharpness of the resonance was attributed by the latter authors to strong exchange interactions between radicals.¹⁰ Hutchison, Pastor, and Kowalsky¹¹ resolved hyperfine structure for hydrazyl dissolved in benzene. Dilution to approximately 0.001 M was found necessary in order to minimize dipolar and exchange interactions which would otherwise obscure the hyperfine structure. They observed five equally spaced components (10-gauss intervals, five-gauss half-widths) which they attributed to equal interactions with the two central nitrogen nuclei. Schneider¹² studied the resonance of hydrazyl dispersed in solidified plastics (1% solutions in perspex

⁷ S. Goldschmidt and K. Renn, *Ber. deut. chem. Ges.* **55**, 628 (1922).

⁸ A. N. Holden, C. Kittel, F. R. Merritt, and W. A. Yager, *Phys. Rev.* **77**, 147 (1950).

⁹ C. H. Townes and J. Turkevich, *Phys. Rev.* **77**, 148 (1950).

¹⁰ J. H. Van Vleck, *Phys. Rev.* **74**, 1168 (1948); M. H. L. Pryce and K. W. H. Stevens, *Proc. Phys. Soc. (London)* **A63**, 36 (1950).

¹¹ C. A. Hutchison, R. C. Pastor, and A. G. Kowalsky, *J. Chem. Phys.* **20**, 534 (1952). Similar results for hydrazyl were reported later by Jarrett (see footnote 17) and by Kikuchi and Cohen (see footnote 18).

¹² E. E. Schneider, *Discussions Faraday Soc.* **19**, 158 (1955).

and in polystyrene) as well as in liquid solvents. He observed quintets in both liquid and solid solutions with spacings of 10 and 20 gauss, respectively. The increased splitting in the solid was attributed to the appearance of the anisotropic terms. Van Roggen, *et al.*^{12a} have also studied dilute solutions of hydrazyl in liquid and frozen benzene.

Most recently, Holmberg, Livingston, and Smith¹³ have observed the resonance of small concentrations of hydrazyl in oriented crystals of the parent hydrazine. They have thereby assigned values to both the isotropic and anisotropic hyperfine parameters. However, since these assignments are based on measurement of integrated ESR absorption, rather than on its derivative, we do not believe them to be as reliable quantitatively as ours. This conclusion is further supported by the fact that the isotropic constants assigned to the solid are completely different from those in solution—a result which we consider inadmissible.

Evidence for hyperfine coupling with the protons in hydrazyl was found by Beljers, *et al.*¹⁴ They observed enhancement of the proton resonance when the electron spin resonance was saturated (Overhauser effect). Resolution of the proton hyperfine structure has recently been achieved by Deguchi¹⁵ by using oxygen-free solvents.^{15a}

Carbazyl was first synthesized by Turkevich; its resonance in the crystalline state was observed by Cohen, Kikuchi, and Turkevich.¹⁶ Jarrett¹⁷ and Kikuchi and Cohen¹⁸ studied its resonance in dilute solution and obtained seven resolved peaks. This pattern was shown to be consistent with the supposition that the hyperfine coupling constants of the two nitrogen atoms are in approximately 2:1 ratio.

Of considerable pertinence to our work are the papers of Weissman and co-workers¹⁹⁻²¹ on the paramagnetic ion peroxyamine disulfonate $(\text{SO}_3)_2\text{NO}^-$. The hyperfine structure of this ion is due entirely to the nitrogen nucleus. This we might regard as the isolation of one of the interactions present in the hydrazyl radicals. In liquid solution a triplet with 13-gauss interval is observed.¹⁹ At concentrations of 0.001 *M* in chloroform the individual linewidth is reduced to less than

0.5 gauss (full width).²⁰ Weissman and Banfill²¹ have also observed the resonance of a single crystal of diamagnetic potassium hydroxylamine disulfonate containing a small concentration (0.25 mole %) of dispersed $(\text{SO}_3)_2\text{NO}^-$. A highly anisotropic spectrum was reported with triplet interval varying between the limits of 6 and 27 gauss.

On the basis of our theory (Sec. II), these results may be very easily explained. If we assign the parameters $|A|=13$ gauss, $|B|=7$ gauss with the same sign as *A*, $C \approx 0$, then the single crystal resonances will always fall in the field range $|A-B|M=6$ gauss to $|A+2B|M=27$ gauss. A particularly gratifying feature is the fact that the spectrum is consistent with $C \approx 0$.²² Thus the distribution of the unpaired electron in the neighborhood of the nitrogen nucleus is very nearly cylindrically symmetrical. We shall assume that this holds true also around the two central nitrogen nuclei in hydrazyl and carbazyl. Thus the specializations of the theory for local cylindrical symmetry shall pertain. We shall also suppose, initially for convenience in computation, that the symmetry axes for the two charge distributions are more or less parallel. The essential consistency of the observed spectra with this hypothesis (see Secs. VI, VIII) does indeed justify its validity. We note further that, since orbitals containing principally *s* and *p* character are prolate, then $B > 0$ for nitrogen hyperfine couplings. For peroxyamine disulfonate we have consequently $A > 0$. Our analysis shall establish also, for hydrazyl and carbazyl, that both isotropic coupling constants are positive (presuming both *B*'s are positive). It has been established experimentally that the isotropic coupling constants are positive for atomic nitrogen²³ and for nitric oxide.²⁴ Thus a rather consistent pattern emerges with regard to the signs of nitrogen coupling constants. We shall return to this discussion on a more quantitative level in Sec. IX.

It was assumed in Sec. II that anisotropy in the *g* tensor could be neglected. We shall now see how closely this idealization is realized. Kikuchi and Cohen,¹⁸ using single crystals, found that the range of variation in *g* with orientation amounts to 2.4 gauss in carbazyl and ~ 1 gauss in hydrazyl (both at 9400 Mc). Livingston and Zeldes^{24a} report 1.2 gauss for the latter. Figures 14 and 15 of footnote 18 indicate very clearly how the anisotropy in *g* affects polycrystalline spectra. Principally, it contributes an additional source of broaden-

^{12a} A. von Roggen, L. van Roggen, and W. Gordy, *Phys. Rev.* **105**, 50 (1957).

¹³ R. W. Holmberg, R. Livingston, and W. T. Smith, *J. Chem. Phys.* **33**, 541 (1960).

¹⁴ H. G. Beljers, L. Van der Kint, and J. S. Van Wieringen, *Phys. Rev.* **95**, 1683 (1954).

¹⁵ Y. Deguchi, *J. Chem. Phys.* **32**, 1584 (1960).

^{15a} Our hydrazyl line shapes accordingly represent envelopes of the fully resolved proton hyperfine structures.

¹⁶ V. W. Cohen, C. Kikuchi, and J. Turkevich, *Phys. Rev.* **85**, 379 (1952).

¹⁷ H. S. Jarrett, *J. Chem. Phys.* **21**, 761 (1953).

¹⁸ C. Kikuchi and V. W. Cohen, *Phys. Rev.* **93**, 394 (1954).

¹⁹ G. E. Pake, J. Townsend, and S. I. Weissman, *Phys. Rev.* **85**, 682 (1952); **89**, 606 (1953).

²⁰ T. L. Chu, G. E. Pake, D. E. Paul, J. Townsend, and S. E. Weissman, *J. Phys. Chem.* **57**, 504 (1953).

²¹ S. I. Weissman and D. Banfill, *J. Am. Chem. Soc.* **75**, 2534 (1953).

²² When $C \neq 0$, the range of resonance contains the three field values $|A+2B|M$, $|A-B+C|M$, and $|A-B-C|M$. This set contains both the largest and the smallest field value of the theoretical line shape, as may be deduced from Eq. (10). Given that the two extremes are 6 and 27 gauss and that $|A|=13$ gauss, it is impossible to choose a consistent set *A*, *B*, *C* unless $C=0$.

²³ L. W. Anderson, F. M. Pipkin, and J. C. Baird, *Phys. Rev.* **116**, 87 (1959).

²⁴ R. Beringer and J. G. Castle, *Phys. Rev.* **78**, 581 (1950); R. Beringer, E. B. Rawson, and A. F. Henry, *ibid.* **94**, 343 (1954).

^{24a} R. Livingston and H. Zeldes, *J. Chem. Phys.* **24**, 170 (1956).

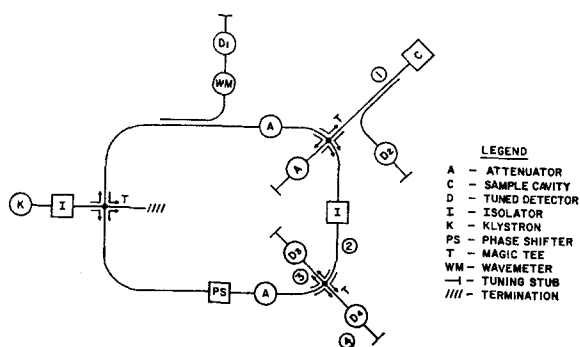


FIG. 3. Balanced bolometer detection system.

ing with half-width 1–2 gauss. In pure polycrystalline samples of these radicals the g anisotropy determines the line shape. The lines are then somewhat asymmetric, the peak being as much as 1 gauss removed from the centroid. However, in dilute solid solutions, where exchange interactions are eliminated and gaussian broadening mechanisms come into play, the symmetry of the polycrystalline profiles is effectively restored. For hydrazyl at least, no asymmetry can be detected in our solid line shapes (see Figs. 7 and 8). In fluid media, of course, the g anisotropy averages out in the same way as the hyperfine anisotropy.

It is not known with certainty which coupling constant is associated with which nitrogen in either hydrazyl or carbazyl. There is some theoretical justification for one particular choice, as will be seen in Sec. IX. An unambiguous assignment could be made through isotopic substitution with N^{15} , as suggested by Hutchison¹¹ and others. In this paper we shall arbitrarily label the larger coupling constants with the subscript 1, the smaller with the subscript 2.

IV. EXPERIMENTAL

Preparation of the Free Radicals²⁵

The precursor substances, diphenylpicrylhydrazine (mp 176°C) and picrylaminocarbazole (mp 238°C), were oxidized with finely divided PbO_2 to the corresponding free radicals. The reactions were carried out immediately before each resonance measurement. Benzene or chloroform was generally used as the solvent. It was also found possible to use silicone fluid for low concentrations of radical. The solid solutions were prepared by initially dissolving the crystalline radicals in polymerizing fluids (Duco cement or Lucite). Hydrazyl was recrystallized from benzene-hexane solution and gave an mp of 129°C. Carbazyl was obtained by evaporation of the solvent and had an mp range of 205–215°C.

²⁵ All samples of hydrazyl and carbazyl were synthesized by Martin L. Peller and Monica R. Nees in this laboratory.

Microwave Detection

To observe ESR absorption we used a balanced-bolometer homodyne system²⁶ operating at around 9300 Mc. This system is shown schematically in Fig. 3. The klystron frequency could be stabilized to either the sample cavity resonance or that of the reference wave meter using D_1 or D_2 . For the present set of experiments the sample cavity resonance was used. Microwave energy at levels between 1 and 10 mw is sent through arm 1 to the sample through the cavity iris. The latter is small enough to keep the cavity slightly undercoupled. The reflected signal goes back through Magic Tee A ; the isolation arm 2 is superposed on the reflection from the tuned arm of the bridge. The bridge is balanced in order to give in arm 2 a small signal proportional to the change in cavity absorption due to magnetic resonance. The signal in arm 2 is now split equally at Magic Tee B and goes to arms 3 and 4 where it is mixed with about 16 mw of coherent microwave energy from the klystron. Thus the original signal from arm 2 is amplified. The bolometers present a signal proportional to $V\Delta V$, V being the signal voltage in arms 3 and 4 and ΔV , the voltage change caused by the change in sample cavity absorption during resonance. The phase of the large coherent signal V is adjusted to match that of ΔV , the signal in arm 2. The dc bias power on the bolometers is also 16 mw in accordance with the conditions for optimum sensitivity (bias power equal to rf power, their sum as high as bolometers will take without burning out). The two elements in what is effectively a tunable balanced mixer operate in push-pull into a transformer circuit which matches their impedance to that of a hushed transistor amplifier (noise figure 3 db). The signal is finally amplified, rectified and recorded using conventional apparatus.

Magnetic Field and ESR Recording

The sample cavity, operating in the TE_{102} mode, is placed between the poles of a Varian 4012-3B magnet with the broad face parallel to the pole face. The sample pole is the center of the short face with the sample in a 4-mm quartz tube lying in the nodal plane of the E field. By means of small coils rigidly attached onto the broad faces of the cavity, the magnetic field is sinusoidally modulated at a frequency of 100 cps with amplitude in the range 2.5–10 gauss. The detection amplifiers are tuned to 100 cps and thus present a signal proportional to the field derivative of the magnetic resonance absorption. Phase demodulation to a recorded dc voltage is effected in a special self-balanced diode circuit²⁷ with an output filter network

²⁶ G. Feher, Bell System Tech. J. **36**, 449 (1957).

²⁷ R. E. Gorozdos and R. L. Konigsberg, The Johns Hopkins University Applied Physics Laboratory, Technical Rept. CM-913, September, 1957.

limiting the signal bandwidth to 0.1–10 cps. The steady magnetic field is swept triangularly back and forth at 1 cps. This reversal eliminates errors due to response lags in the train of detection circuits. Precise measurements of the field were obtained by means of a proton resonance probe a few centimeters from the sample.

V. HYDRAZYL IN FLUID

Dilute solutions (approximately 0.001 *M*) of hydrazyl in benzene, chloroform, and silicone fluid exhibited practically identical spectra. No influence of anisotropic hyperfine interaction was apparent. Figure 4 shows a typical spectrum in benzene solution. The

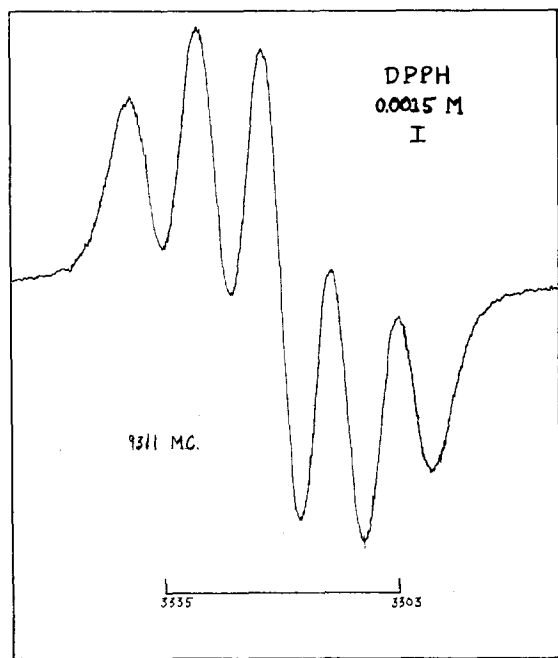


FIG. 4. Resonance of hydrazyl in benzene solution.

five-peak pattern is in qualitative agreement with earlier work on dilute solutions of hydrazyl.^{11,16,17} Hutchison, Pastor, and Kowalsky¹¹ had attributed this spectrum to approximately equal isotropic interactions with the two nitrogens, estimating that

$$|A_1| \approx |A_2| \approx 10 \text{ gauss.}$$

By a more detailed analysis of the spectrum, outlined below, we have been able to make more exact assignments of the isotropic coupling constants. The underlying pattern for the isotropic hyperfine splitting is shown in Fig. 5. It is apparent that the intervals between centroids of the fine line clusters are equal even when the two constants $|A_1|$, $|A_2|$ are different. The width of each cluster does, however, depend on $|A_1| - |A_2|$. We denote by σ^* the second moment of a line cluster and by σ the Gaussian half-width of each com-

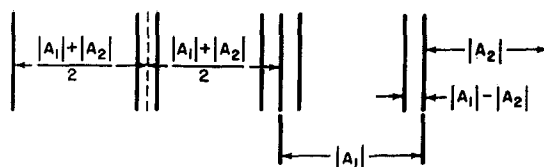


FIG. 5. Basic pattern for isotropic hyperfine interaction in hydrazyl.

ponent line (presumed all equal). It may be shown that

$$\sigma_2^* = [\sigma^2 + \frac{1}{4}(|A_1| - |A_2|)^2]^{\frac{1}{2}} \quad (22)$$

for a two-component cluster and

$$\sigma_3^* = [\sigma^2 + \frac{2}{3}(|A_1| - |A_2|)^2]^{\frac{1}{2}} \quad (23)$$

for a three-component cluster. Furthermore, in both cases, σ^* is very nearly equal to the distance from centroid to point of maximum slope in a line cluster, indicating that the cluster shape is also essentially gaussian.

The over-all line shape was accordingly represented by a superposition of five equally-spaced Gaussians in intensity ratio 1:2:3:2:1 with half-widths σ , σ_2^* , σ_3^* , σ_2^* , σ , respectively. The following choice of parameters was found to best reproduce the experimental line shape:

$$|A_1| = 9.35 \pm 0.20 \text{ gauss,}$$

$$|A_2| = 7.85 \pm 0.20 \text{ gauss,}$$

$$\sigma = 3.36 \pm 0.20 \text{ gauss.}$$

The synthesized resonance spectrum with these parameters is drawn in Fig. 6. Here, and in what follows, the limits of error are estimated by constructing curves for neighboring values of the parameters. The cluster approximation agrees very closely with the rigorous nine-Gaussian line shape corresponding to the same constants (the latter used for Fig. 6).

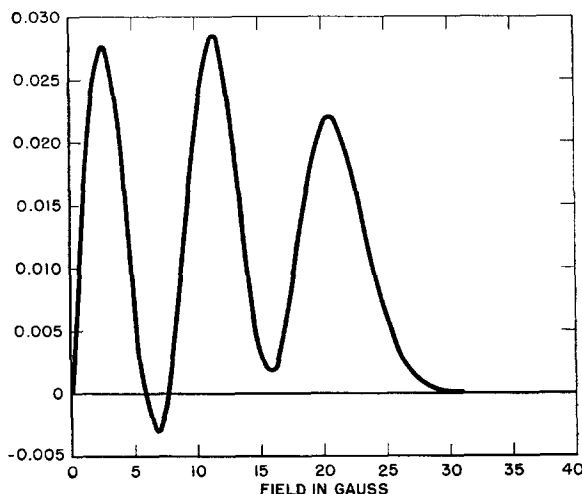


FIG. 6. Hydrazyl in liquid: theoretical resonance line shape.

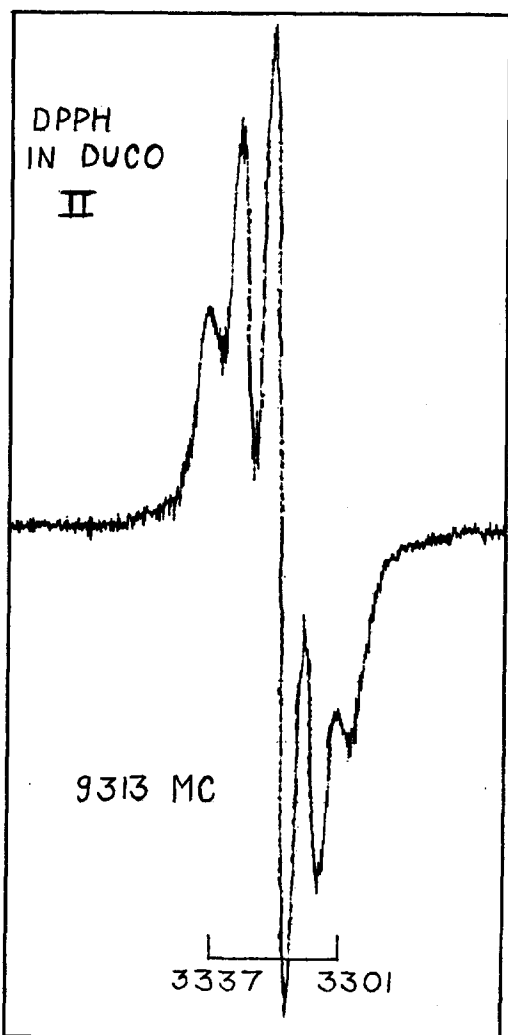


FIG. 7. Resonance of hydrazyl in semifluid Duco cement. (The observation was made one day after the solution was prepared.)

Recently, Deal and Koski²⁸ have reported a determination of the ratio $|A_2/A_1|=0.82$ in close accord with our value of 0.84. No estimates of the coupling constants themselves are given by these authors.

VI. HYDRAZYL IN SOLID

Figure 7 shows the spectrum of hydrazyl dispersed in semi-fluid Duco cement. Here the anisotropic hyperfine terms begin to manifest themselves, indicating hindrance to molecular motions in the increasingly viscous medium. A detailed discussion of the fluid-solid transition is given in the next section. Eventually, the Duco hardens completely (as the acetone solvent evaporates) and the spectrum shown in Fig. 8 is observed. It is assumed that the hydrazyl radicals are here completely frozen in random orientations. The

resonance line shape should thereby be governed by the theory of Sec. II. The solid spectrum is considerably more difficult to analyze than the liquid spectrum. Relative signs as well as magnitudes of the four interaction constants are now significant. We note that the spectrum retains its five-peak structure, the components being, however, broadened and their spacing increased to about 21 gauss. It was originally supposed that these peaks corresponded to the maxima in the solid spectra, i.e., to the frequencies $|A-B|M$, etc. This would lead to values for B in the neighborhood of 12 gauss with opposite signs from the A 's.²⁹ These constants, in addition to being rather implausible on theoretical grounds, do not provide an accurate fit of the experimental derivative spectrum, particularly as concerns the widths of the individual lines. If, on the other hand, the solid peaks (exclusive of the central one) are presumed to correspond to the $|A+2B|M$ ends of the component lines, then an excellent fit of the experimental spectrum may be obtained. The optimal

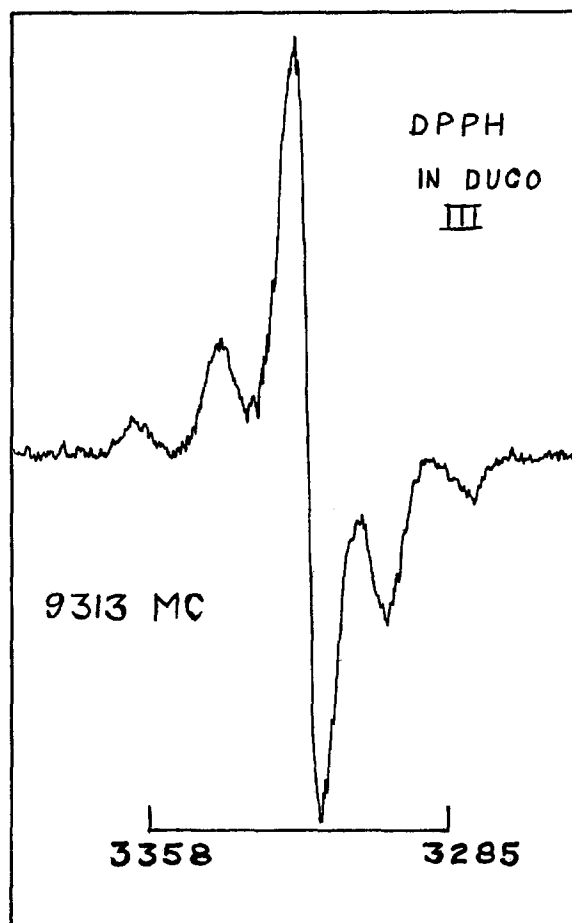


FIG. 8. Resonance of hydrazyl in hardened Duco cement.

²⁹ Such an assignment was reported by us during a preliminary stage of this work: N. W. Lord and S. M. Blinder, *Bull. Am. Phys. Soc.* **5**, 72 (1960).

²⁸ R. M. Deal and W. S. Koski, *J. Chem. Phys.* **31**, 1138 (1959).

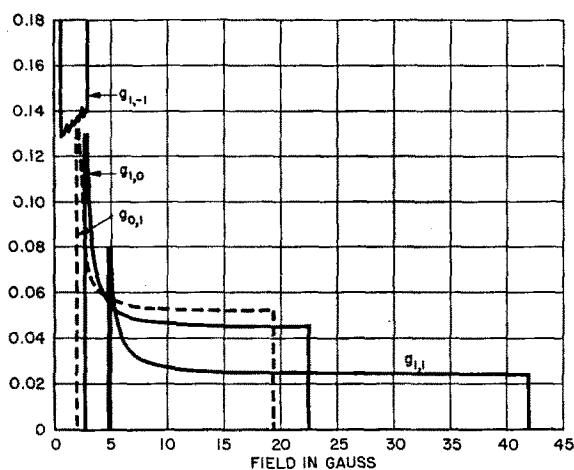


Fig. 9. Hydrazyl in solid: components of theoretical line shape.

set of constants determined in this fashion is:

$$A_1 = 9.35 \pm 0.20 \text{ gauss};$$

$$A_2 = 7.85 \pm 0.20 \text{ gauss};$$

$$B_1 = 6.6 \pm 0.5 \text{ gauss};$$

$$B_2 = 5.8 \pm 0.5 \text{ gauss}.$$

The uncertainty in the anisotropic parameters is larger since, in addition to the solid analysis being more tedious, any error in the isotropic parameters is compounded.

Each isotropic parameter has the same sign as its corresponding anisotropic parameter. Since it is highly probable that both B 's are positive (see Sec. III), all four hyperfine coupling constants are almost certainly positive. The ambiguity in the signs of the isotropic parameters is thereby removed. The components of the theoretical line shape (with no Gaussian broadening)

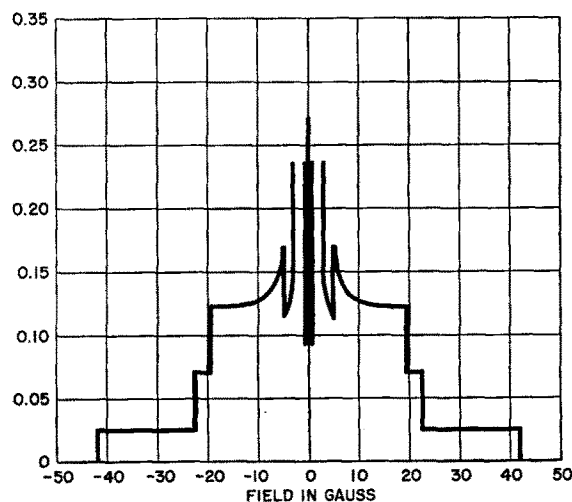


Fig. 10. Hydrazyl in solid: theoretical line shape.

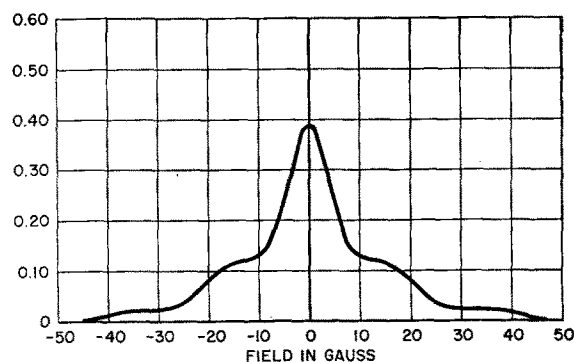


Fig. 11. Hydrazyl in solid: theoretical line shape with Gaussian broadening.

are drawn in Fig. 9. Figure 10 shows the complete theoretical profile. The outer edges of the g_{01} and g_{10} component functions are quite close together, which accounts for the five-line structure of the solid spectrum. The solid line shape is also critically dependent on the Gaussian broadening parameter. It is noteworthy that an excellent fit can be obtained by using the liquid value, $\sigma = 3.36$ gauss, for each component line in the solid. This would indicate that the principal source of line broadening is the same in both phases, presumably unresolved hyperfine interaction with the other magnetic nuclei. The Gaussian transform of the

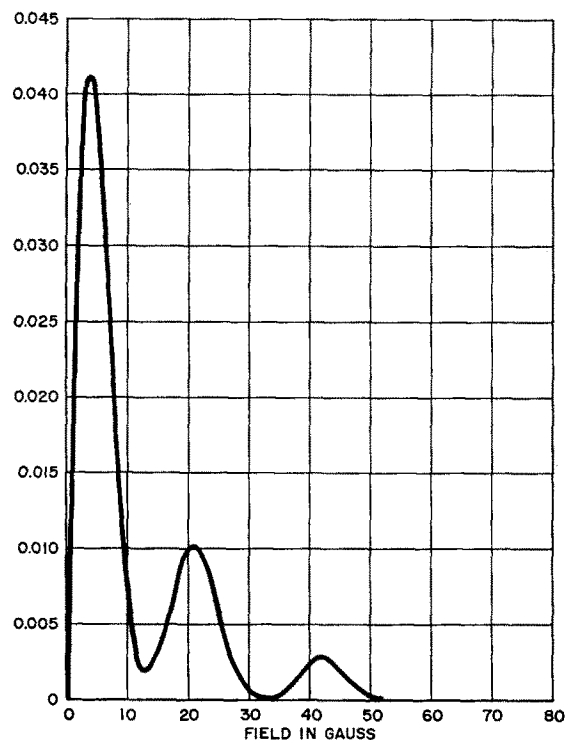


Fig. 12. Hydrazyl in solid: derivative of theoretical line shape. (This is the theoretical construction of the spectrum shown in Fig. 8.)

theoretical line shape is shown in Fig. 11 and its derivative in Fig. 12. The latter is then the theoretical construction of the observed spectrum Fig. 8.

To summarize, three parameters B_1 , B_2 , and σ were fitted to theoretical line shapes such as Eq. (19) so as to give the best possible reproduction of the spectrum in Fig. 8. The isotropic parameters, A_1 , A_2 were presumed to remain constant during the fluid-solid transition. The quantitatively excellent agreement between theory and experiment constitutes *a posteriori* verification for the hypotheses of local cylindrical symmetry and near parallelism of axes.

VII. HYDRAZYL. INTERMEDIATE STATE

We shall now discuss in greater detail the hyperfine structure of the resonance during the transition from liquid to solid solution. The nature of the medium manifests itself in spin-resonance experiments in the mode of averaging the spin Hamiltonian over its orientation variables. Presuming that such molecular motions are governed by the theory of random processes,³⁰ the medium may be characterized by a correlation time τ_c . This parameter represents some effective average time during which a molecular orientation persists, or alternatively, the average time between reorienting collisions. A well-known application of this concept was made by Debye³¹ in his study of dielectric dispersion in polar liquids. The importance of the correlation time in magnetic resonance was made evident by the work of Bloembergen, Purcell, and Pound.³²

In our case, the orientation-dependent features of the spectra are governed by the relative magnitude of τ_c and \hbar/A , the latter being roughly the period of nuclear Larmor precession. The two extreme cases, $\hbar/A \gg \tau_c$ and $\tau_c \gg \hbar/A$ characterize the liquid and solid states respectively. These present no difficulties in analysis or interpretation. The intermediate case, in which τ_c and \hbar/A become comparable, is a different matter entirely. A very viscous fluid would fall in this category.³³ Theory must now account for the exceedingly complex interplay of hyperfine interactions and molecular motions of comparable frequency.

McConnell,³⁴ following the approach of Bloembergen, Purcell, and Pound, gave an approximate analysis of

³⁰ Excellent reviews of physical applications of random function theory are given by S. Chandrasekhar, *Revs. Modern Phys.* **15**, 1 (1943) and by M. C. Wang and G. E. Uhlenbeck, *ibid.* **17**, 323 (1945).

³¹ See, for example, P. Debye, *Polar Molecules* (Dover Publications, New York, 1945), Chap. V.

³² N. Bloembergen, E. M. Purcell, and R. V. Pound, *Phys. Rev.* **73**, 679 (1948).

³³ According to Bloembergen, Purcell, and Pound, the viscosity is related to the correlation time by

$$\tau_c \approx 4\pi\eta a^3/3kT,$$

where a is the effective Stokes' law radius. When $\tau_c \sim \hbar/A$, the viscosity of our hydrazyl-Duco solution is thus of the order of 100 cp.

³⁴ H. M. McConnell, *J. Chem. Phys.* **25**, 709 (1956).

the intermediate state as applied to line breadth. Analogous procedures applied to explicit computation of resonance line shapes for intermediate states would, however, prove prohibitively difficult. Moreover, there arises a more fundamental question as to whether it is valid to regard molecular orientations as being instantaneously determinate in the classical sense. A rigorous quantum-mechanical approach³⁵ would necessitate extension of the Hamiltonian to include the effects of molecular reorientations and collisions. The random nature of the latter interactions might then be taken into account by some quantum-statistical technique. In the absence of any full treatment, along either classical or quantum-mechanical lines, we are forced to seek some less exact model to account for the effects of random molecular motion.

To facilitate our treatment, we rewrite the hyperfine interaction terms of the spin Hamiltonian (1) in the form

$$\mathcal{U}(M_S, \mathbf{I}) = M_S \{ \alpha(\Omega) I_x + \beta(\Omega) I_y + [A + \gamma(\Omega)] I_z \}, \quad (24)$$

where $\alpha(\Omega)$, $\beta(\Omega)$ and $\gamma(\Omega)$ are functions of molecular orientation and of the anisotropic parameters B and C . The explicit forms of α , β and γ are given in footnote 5. For the present, we need only know that

$$\int d\Omega \alpha(\Omega) = \int d\Omega \beta(\Omega) = \int d\Omega \gamma(\Omega) = 0, \quad (25)$$

and that α , β , and γ are linear and homogeneous in B and C . The averages of these functions for some particular mode of molecular motion are denoted by $\langle \alpha \rangle_{Av}$, $\langle \beta \rangle_{Av}$, and $\langle \gamma \rangle_{Av}$. Representing the relative probability of an orientation Ω during a time \hbar/A by the distribution function $\rho(\Omega)$, we have

$$\langle \alpha(\Omega) \rangle_{Av} = (1/4\pi) \int d\Omega \rho(\Omega) \alpha(\Omega), \quad (26)$$

and similarly for β and γ . When $\hbar/A \gg \tau_c$, all elements of solid angle are available to the molecule many times over and with equal probability during an interval \hbar/A . The distribution function is spherically symmetrical and when normalized,

$$\rho_0(\Omega) = 1,$$

the subscript 0 being used to label the liquid state. The averages $\langle \alpha(\Omega)_0 \rangle_{Av}$, $\langle \beta(\Omega)_0 \rangle_{Av}$, and $\langle \gamma(\Omega)_0 \rangle_{Av}$ are just the integrals (25) and all vanish. Thus the hyperfine operator in liquids assumes the simple form

$$\langle \mathcal{U}_0 \rangle_{Av} = A M_S I_z. \quad (27)$$

In the opposite extreme $\tau_c \gg \hbar/A$ each molecule is restricted to a small range of solid angle. We idealize the latter as a single orientation Ω_k , differing, in general,

³⁵ Probably beyond the scope of present theoretical understanding of the liquid state.

for each molecule k , and write

$$\rho_1(\Omega) = \delta(\Omega - \Omega_k),$$

the subscript 1 denoting the solid state. We find then that

$$\langle \alpha(\Omega)_1 \rangle_{\text{av}} = \alpha(\Omega_k), \quad \text{etc.} \quad (28)$$

By superposition of the ensemble distribution of hyperfine interactions (for all orientations Ω_k) we arrive at the polycrystalline spectra of Sec. II.

We are faced now with a choice of some parametric representation of the continuum of intermediate states. To this end, we postulate that there exists a parameter λ ($0 \leq \lambda \leq 1$) which characterizes the degree of transition from the liquid to the solid state. More concretely, we assume that the distribution function for the intermediate state depends linearly on λ . Accordingly, we have

$$\begin{aligned} \rho_\lambda(\Omega) &= (1-\lambda)\rho_0(\Omega) + \lambda\rho_1(\Omega) \\ &= 1 - \lambda + \lambda\delta(\Omega - \Omega_k). \end{aligned} \quad (29)$$

Integration over Ω yields the averages

$$\langle \alpha(\Omega)_\lambda \rangle_{\text{av}} = \lambda\alpha(\Omega_k), \quad \text{etc.} \quad (30)$$

The term in A remains unchanged. Recalling that α , B , γ are linear and homogeneous in B and C , it follows that

$$\lambda\alpha_{B,C}(\Omega_k) = \alpha_{\lambda B, \lambda C}(\Omega_k), \quad \text{etc.} \quad (31)$$

We obtain thereby the key result that the polycrystalline solid line-shape formulas apply as well to the intermediate state provided that we make the substitutions

$$B \rightarrow \lambda B$$

$$C \rightarrow \lambda C.$$

Thus, in the case of cylindrical symmetry, for interaction with a single magnetic nucleus, the normalized line shape is given by

$$g_{M,\lambda}(\nu) = \frac{1}{M} \frac{\nu/M}{|6A\lambda B + 3\lambda^2 B^2|^{3/2} |(\nu/M)^2 - (A - \lambda B)^2|^{3/2}} \quad (32)$$

the range of resonance being

$$|A - \lambda B| M \quad \text{to} \quad |A + 2\lambda B| M.$$

For interactions with more than one nucleus, one would expect the corresponding λ coefficients to be the same.

A possible physical interpretation of our parametrization is that $1 - \lambda$ represents the fraction of solid angle accessible to some representative molecule during some typical time interval h/A .

It was found possible to fit the resonance line shape for hydrazyl in partially hardened Duco (Fig. 7) to a theoretical curve (Fig. 13) corresponding to $\lambda = 0.25 \pm 0.02$. Apparently, the hydrazyl sample has made roughly one-fourth the transition from liquid to solid, insofar

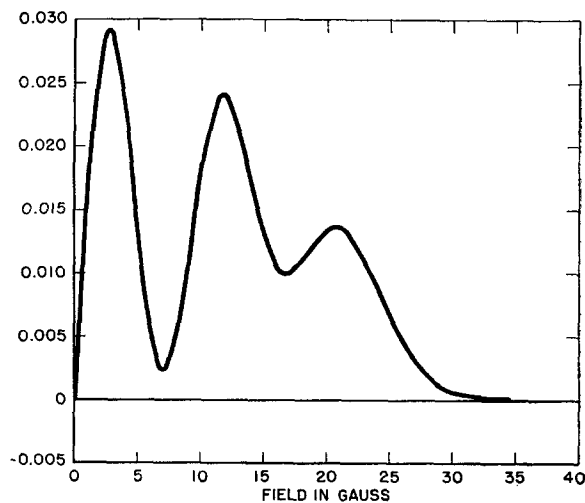


FIG. 13. Hydrazyl intermediate state: theoretical resonance line shape $\lambda = 0.25$. (This is the theoretical synthesis of the spectrum Fig. 7.)

as magnetic resonance constitutes a gauge. The impressive concordance between the experimental and the fitted resonance line shapes lends weighty support to our model for the intermediate state. Secondly, further verification is provided for our assignment of hyperfine coupling constants, as will be seen more explicitly in the following paragraph.

The shape of a single hyperfine component undergoing incipient broadening remains practically gaussian until the line breadth (from angular dependence of hyperfine structure) becomes comparable with the gaussian σ . The second moment of the line is closely approximated, for small λ , by $[\sigma^2 + \frac{3}{4}\lambda^2 B^2 M^2]^{1/2}$. The centroid of the component line shifts from AM in the liquid to $[A^2 - \frac{1}{2}A\lambda B + \frac{7}{4}\lambda^2 B^2]^{1/2} M$. If A and B are of the same sign, this initial shift is inward (towards the center of the resonance). In our intermediate spectrum the peaks shift inward precisely as predicted thus providing independent proof that both pairs A_i , B_i have the same sign.

For the spectrum Fig. 7 the approximation that the broadened lines remain Gaussian was found quite adequate despite the rather large value of λ . The synthesized spectrum (Fig. 13) was nevertheless computed rigorously, as were the solid state curves (Sec. VI). As λ increases further we should expect each peak to split into two, corresponding to the two frequencies $|A - \lambda B| M$ and $|A + 2\lambda B| M$. Naturally, not all of these would be observable because of overlapping. As shown in Sec. VI, only peaks corresponding to the $|A + 2\lambda B| M$ survive after complete solidification of the matrix containing hydrazyl.

VIII. CARBAZYL IN FLUID AND SOLID MEDIA

A procedure analogous to that of Secs. V and VI was followed with carbazyl. Resonance of a dilute solution of carbazyl in benzene is illustrated in Fig. 14. An

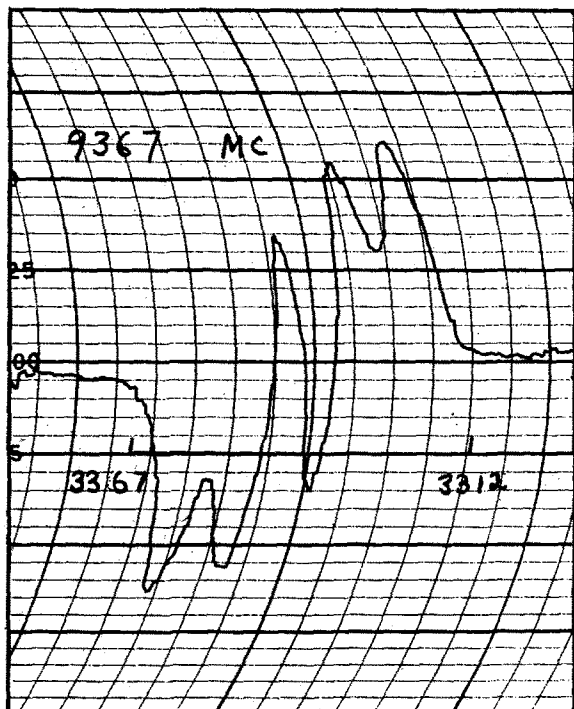


FIG. 14. Resonance of carbazyl in benzene solution.

identical spectrum was obtained in chloroform solution. Again, there is no evidence of any anisotropic interaction. Consistent with earlier studies^{17,18} a seven-line pattern is observed. This had been attributed to isotropic hyperfine interaction with $|A_1| \approx 2|A_2|$. Jarrett¹⁷ gives the value 37.3 Mc (13.3 gauss) for the larger constant.³⁶ Kikuchi and Cohen¹⁸ estimate that the interval is $\frac{5}{8}$ that of hydrazyl, which is equivalent to $|A_1| = 10.8$ gauss using our hydrazyl data.

Figure 15 shows the basic pattern for the isotropic hyperfine structure of carbazyl. The relationships among the various spacings are evident from the diagram. Representing the line shape by a sum of nine gaussians, we obtain the best fit with the parameters:

$$|A_1| = 10.2 \pm 0.5 \text{ gauss};$$

$$|A_2| = 5.8 \pm 0.5 \text{ gauss};$$

$$\sigma = 3.4 \pm 0.5 \text{ gauss}.$$

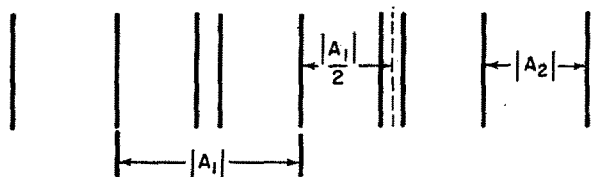


FIG. 15. Isotropic hyperfine structure of carbazyl.

³⁶ The resonance spectrum for carbazyl shown in Fig. 1(b) of Jarrett's paper (see footnote 17) is very similar to ours. Hence, our assignment of parameters is more in accord with his data than are the values quoted by him: $A_1 = 37.3$ Mc (13.3 gauss), $A_2 = 18.6$ Mc (6.6 gauss).

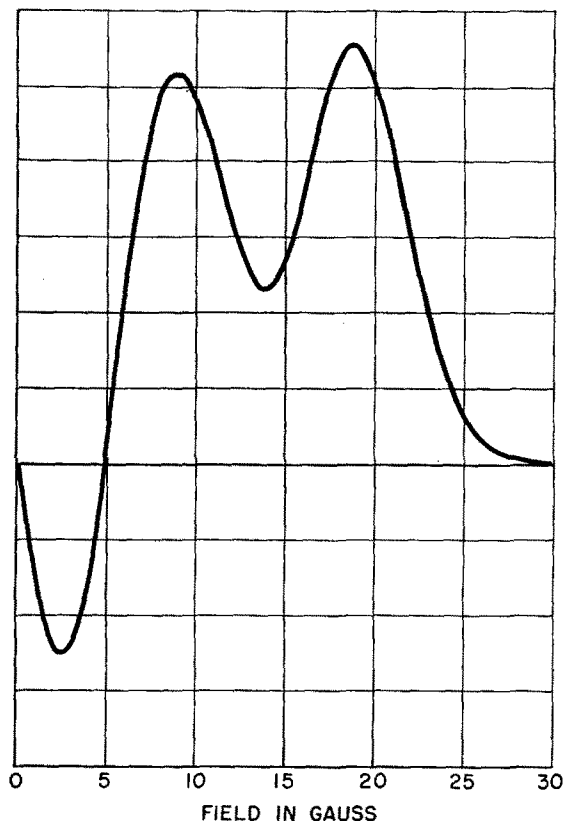


FIG. 16. Carbazyl in liquid: theoretical resonance line shape.

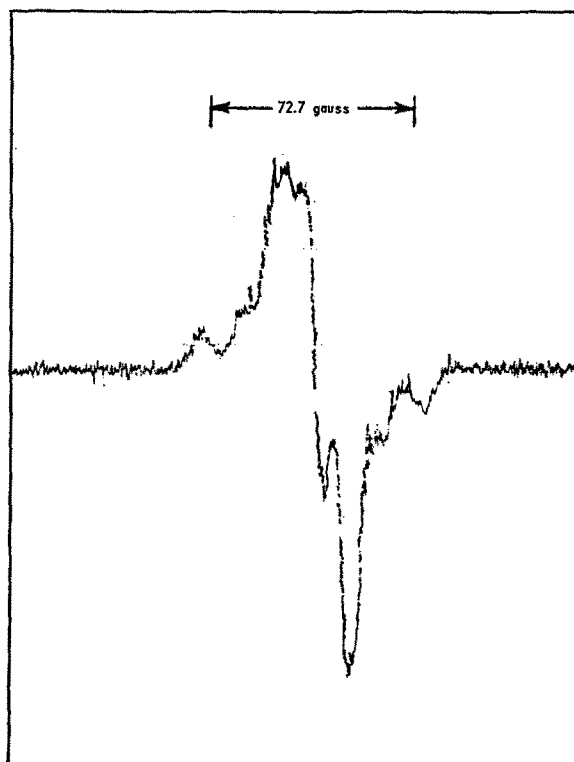


FIG. 17. Resonance of carbazyl in Lucite.

The synthesized derivative is drawn in Fig. 16. Our ratio $|A_2/A_1|$ is 0.57 in contrast with the idealized value of $\frac{1}{2}$.

A trace of the ESR of carbazyl dispersed in the solid is shown in Fig. 17. Methyl methacrylate (Lucite) was used as the trapping matrix. Duco cement is not suitable here since carbazyl is destroyed by reaction with acetone. The asymmetry of the spectrum, Fig. 17, is attributed to the presence of another paramagnetic species in the solid. As shown in Fig. 18, the asymmetric spectrum may be resolved into a sum of two symmetric components with slightly different g factors. The second species has, evidently, an over-all line shape very similar to that of the principal species. The former may be carbazyl which has segregated into small crystallites. The narrowing and g shift would thereby be consequences of enhanced exchange interaction.

We must now construct a theoretical representation of the absorption derivative (solid curve of Fig. 18). As before, the isotropic hyperfine parameters from the liquid are presumed to carry over to the solid. In fitting the two anisotropic parameters to the solid spectra (in hydrazyl as well) it was found possible to employ a two-step procedure with only one variant at a time. First the sum of B_1 and B_2 is fitted to the outermost peak of the resonance, then their ratio is adjusted to best reproduce the other features of the spectrum. The outer peak remains relatively insensitive to variations in the ratio. The parameters chosen in this manner are:

$$A_1 = 10.2 \pm 0.5 \text{ gauss};$$

$$A_2 = 5.8 \pm 0.5 \text{ gauss};$$

$$B_1 = 7.7 \pm 1.0 \text{ gauss};$$

$$B_2 = 4.1 \pm 1.0 \text{ gauss};$$

$$\sigma = 3.4 \pm 0.5 \text{ gauss}.$$

Again, all the parameters are positive, and again the gaussian σ for the liquid applies for the solid.

The steps in the synthesis of the carbazyl line shape, analogous to Figs. 9-12, are drawn in Figs. 19-22. Comparing Figs. 17 and 22, we see that the principal features of the spectrum are reproduced and that the positions of maxima and minima are predicted very closely. The agreement is, however, not so impressive visually as in the case of solid hydrazyl. In rationalization we should note that the carbazyl resonance is more complex than that of hydrazyl. It is also considerably weaker and is thus subjected to a relatively higher noise level. Moreover, an additional step, viz., subtraction of the superposed signal, was necessary to isolate the physically meaningful absorption derivative. Notwithstanding these operational difficulties, there is the possibility that our idealizations, i.e., isotropic g tensor, axial symmetry, and parallel orbitals, are not as closely realized in carbazyl.

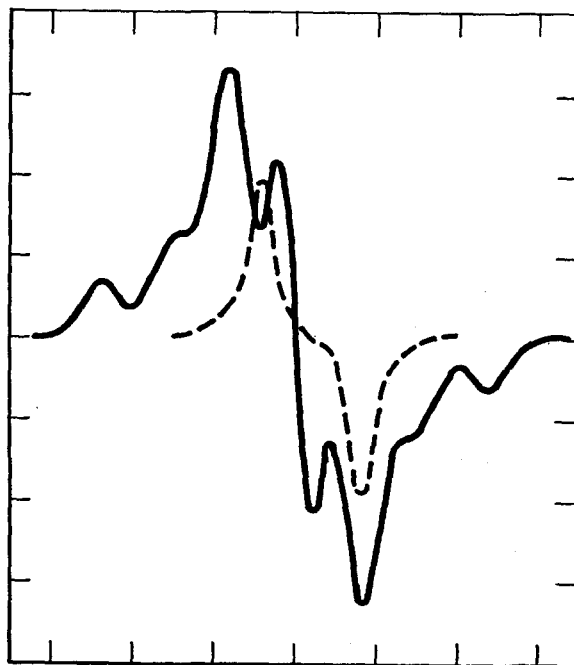


Fig. 18. Synthesis of the asymmetric spectrum of carbazyl in solid.

The implications of the hydrazyl and carbazyl hyperfine spectra with regard to the electronic structure of these radicals will be discussed next.

IX. DISCUSSION

Isotropic and anisotropic hyperfine coupling constants may be represented as integrals over a molecular wave function (see Sec. II). Hence, these parameters contain certain information about the wave function, particularly that part of it describing the unpaired electron. In this section we shall attempt to extract such information as we can from calculated and observed features of the hyperfine structure in hydrazyl and carbazyl.

The essential validity of our model of local cylindrical symmetry (see Sec. III) is borne out by its consistency with the observed spectra (Secs. V-VIII). We conclude that the unpaired spin, in the vicinity of the α and β nitrogen atoms, resides in orbitals having at least approximate cylindrical symmetry (or three-fold axial symmetry). An obvious limitation on cylindrical symmetry is the fact that the proximity of the second spin distribution perturbs the symmetry of the first. For a spin density ρ_i on atom i , a distance 1.46 Å from atom j (see footnote 39), we calculate that $C_j = 0.67\rho_i$ gauss. Thus we have been neglecting individual off-axial contributions of 0.2-0.5 gauss, probably within the uncertainty of the corresponding B parameters.³⁷

We can deduce further that the singly-occupied orbital has principally p character. For an atomic nitrogen $2p$ orbital, the integral (8) yields the value

³⁷ Small deviations from axial symmetry, <1 gauss say, will not radically affect the polycrystalline line shapes.

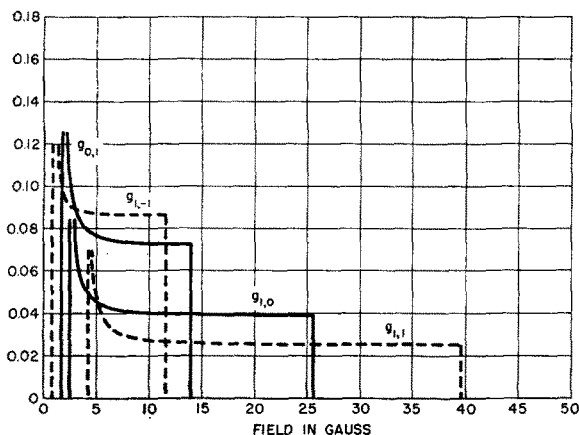


FIG. 19. Carbazyl in solid: components of theoretical line shape.

10.2 gauss for B_N .³⁸ The sum B_1+B_2 is comparable to this for both hydrazyl ($B_1+B_2=12.4$ gauss) and carbazyl ($B_1+B_2=11.8$ gauss).³⁹ The fact that $B_1+B_2 > B_N$ might be attributed to two factors: (i) decrease in the effective nuclear shielding σ when the atom becomes bonded, a consequence of the outward diffusion of charge,⁴⁰ and (ii) the possibility that the sum of the spin densities on N_α and N_β is greater than unity, which could arise from introduction of negative spin densities into other parts of the molecule.⁴¹

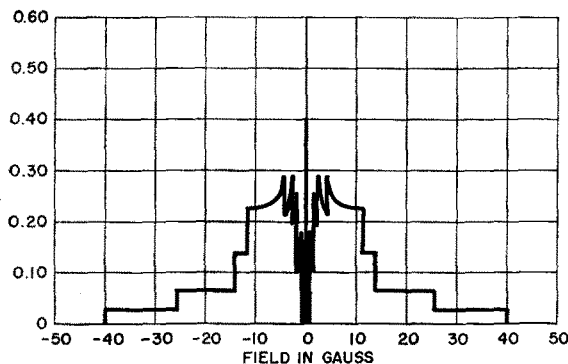


FIG. 20. Carbazyl in solid: theoretical line shape.

³⁸ Using in the integral (8) a hydrogen-like $2p_z$ orbital,

$$\psi(r, \theta) = [4(2\pi)^3]^{-1/2} (Z-\sigma)^{5/2} r \cos\theta \exp[-(Z-\sigma)r/2],$$

where σ is the effective electron shielding parameter, we find

$$B = 0.229(Z-\sigma)^3, \text{ in gauss.}$$

For the $2p$ shell of atomic nitrogen, Hartree gives $\sigma = 3.46$ [D. R. Hartree, *The Calculation of Atomic Structures* (John Wiley & Sons, Inc., New York, 1957), p. 167]. Hence $B_N = 10.2$ gauss.

³⁹ These sums include the effect of interatomic interaction, whereas the corresponding quantities for isolated atoms would be more meaningful for our purposes. A spin density ρ_i on nitrogen atom i decreases B_j by $0.16 \rho_i$ gauss, presuming that the $N-N$ distance is 1.46 \AA , its value in hydrazine. [See T. Moeller, *Inorganic Chemistry* (John Wiley & Sons, Inc., New York, 1952), p. 582]. This contribution is within the uncertainty in the sums, hence is not considered further.

⁴⁰ This effect may be complicated by introduction of net positive or negative charges on these atoms. See resonance structures, Fig. 23.

⁴¹ H. M. McConnell and D. B. Chesnut, *J. Chem. Phys.* **27**, 984 (1957).

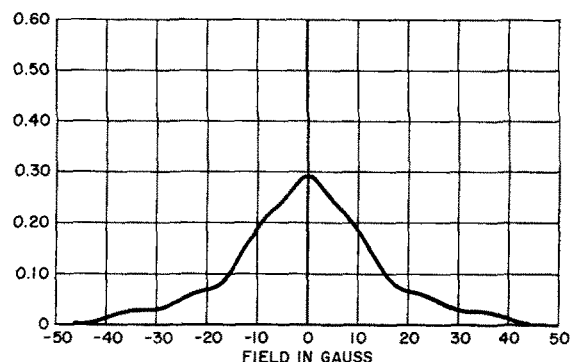


FIG. 21. Carbazyl in solid: theoretical line shape with Gaussian broadening.

The isotropic hyperfine interactions are more difficult to analyze quantitatively since these are due to a combination of two effects: (i) direct contact interaction from admixture of s character into the orbital containing the odd electron, and (ii) spin polarization, resulting in contributions from doubly-occupied orbitals. A prototype of the first effect might be the hyperfine interaction in atomic hydrogen, of the second, that in atomic nitrogen.⁴² The resolution into (i) and (ii) is not unique but depends on the choice of ground state molecular orbital configuration. A single configuration, no matter how expediently chosen, will always have a residual effect (ii) (excepting cases of fortuitous cancellation). Thereby is manifest the fact that a many-electron system cannot rigorously be described by a single MO configuration.

The origin of spin polarization, as pointed out by McConnell and Chesnut,⁴³ may be discussed from three complementary points of view. In the language of molecular orbital theory one would ascribe the effect to configuration interaction with excited molecular states of the same symmetry. Accordingly, the unpaired spin

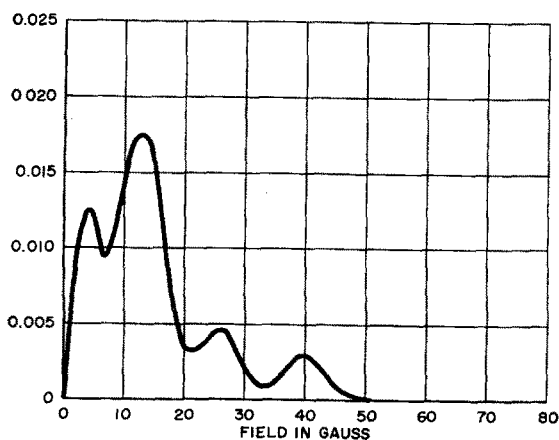


FIG. 22. Carbazyl in solid: derivative of theoretical line shape.

⁴² S. M. Blinder, *Bull. Am. Phys. Soc.* **5**, 14 (1960).

⁴³ H. M. McConnell and D. B. Chesnut, *J. Chem. Phys.* **28**, 107 (1958).

would not reside totally in one particular molecular orbital but would be transmitted partially to other orbitals. Alternately, one might choose to remain within the formalism of a single configuration and attribute the transference of spin to "exchange polarization." Such is the result of the application of the unrestricted Hartree-Fock method⁴⁴ to systems having net spin. Physically, spin polarization is a manifestation of the Exclusion Principle, whereby electrons of the same spin experience mutual repulsions over and above their ordinary electrostatic repulsions. The third mode of description is provided by valence bond theory. Delocalization of spin is here a consequence of resonance among alternative electron pairing schemes. For example, we could write for either of our radicals a set of structures having an unpaired electron localized on the α nitrogen, and another set with one on the β nitrogen. There are, of course, still other structures in which the odd electron is drawn into the ring systems. It is, in fact, the last, which to a large degree enhance the stability of these radicals. We indicate in Fig. 23 representations of the three types of canonical valence-bond structures.

It is clear that the direct contact interaction is rather small in hydrazyl and carbazyl, for an unpaired electron in a pure $2s$ orbital would give a value for A in excess of 600 gauss.⁴⁵ The observed values (6–10 gauss) indicate that the hybridization of the p orbitals can be no greater than 1–2%. Three N_α bond orbitals must then be constructed out of the $2s$ orbital and the remaining two $2p$ orbitals. Such bonds must necessarily lie in the plane perpendicular to the unpaired p orbital. We deduce thereby an important fact about the structure of our two radicals, namely that the three bonds to the α nitrogen lie very nearly in a plane and are, on the average, sp^2 hybrids. In contrast, the corresponding bonds in hydrazine (likewise in ammonia) form a trigonal pyramid.⁴⁶

It is similarly evident that the two bonds to the β nitrogen lie in the same plane, but it is not unambiguously clear whether they are sp^2 hybrids (along with the unshared pair) or colinear sp hybrids, leaving the unshared pair in a p orbital. The latter is favored in view of the several double-bonded resonance structures (Fig. 23).

We know then that the two nitrogen atoms and the three carbon atoms bonded to them all lie in a plane. The well-known criterion for maximum stability in π electron systems suggests further that (neglecting steric effects) the two radicals are planar in their entirety. Therefore, the structural formulas (Fig. 1) as drawn

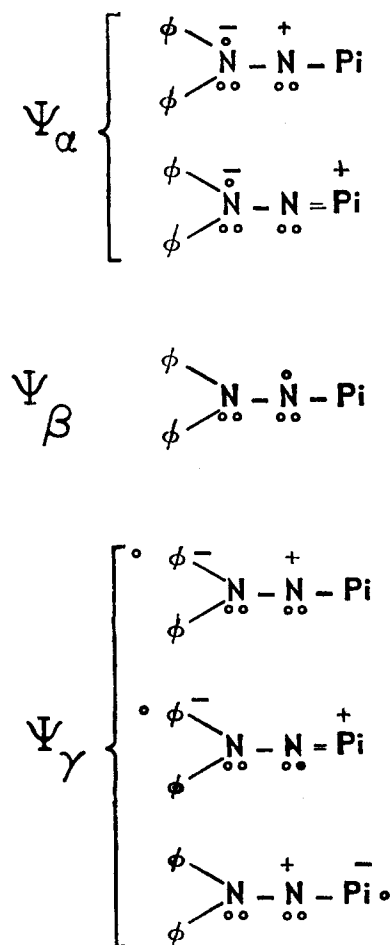


FIG. 23. Some valence bond structures for substituted hydrazyl free radicals.

are probably good representations of the actual geometric configurations of hydrazyl and carbazyl.

Thus far we have established an upper limit on s admixture into the unpaired electron's orbital (1–2%). We consider even this small percentage to be too large for two reasons: (i) From simple energetic considerations, it would be more feasible here that all available s character be used in the bond orbitals so as to maximize their overlap with neighboring atoms.⁴⁷ For instance, in the free radicals CH_3 and NH_2 , isoelectronic with the α and β nitrogen atoms, respectively, the odd electron has pure p character.⁴⁸ (ii) The approximate proportionality of pairs A_i , B_i ⁴⁹ suggests that spin polarization is the dominant mechanism for the isotropic interactions. We note first that the B constants are probably the best measure we have of spin density

⁴⁴ R. K. Nesbet, Proc. Roy. Soc. (London) **A230**, 312 (1955); G. W. Pratt, Phys. Rev. **102**, 1303 (1956).

⁴⁵ This value is calculated from Hartree's SCF wave function for the $2s$ atomic orbital in the nitrogen atom [D. R. Hartree and W. Hartree, Proc. Roy. Soc. (London) **A193**, 299 (1948)].

⁴⁶ F. Moeller, *Inorganic Chemistry* (John Wiley & Sons, Inc., New York, 1952), p. 582.

⁴⁷ See, for example, L. Pauling, *The Nature of the Chemical Bond* (Cornell University Press, Ithaca, New York, 1948), 2nd ed., pp. 86–89; C. A. Coulson, *Valence* (Oxford University Press, London, 1952), Chap. VIII.

⁴⁸ R. S. Mulliken, J. Chem. Phys. **1**, 492 (1933).

⁴⁹ For hydrazyl, $A_1/B_1=1.42$, $A_2/B_2=1.35$; for carbazyl, $A_1/B_1=1.32$, $A_2/B_2=1.41$.

since they involve no indirect interactions. (This presumes that the effective shielding constants σ for the two nitrogens are not overly disparate). It follows then that each A is approximately proportional to its corresponding spin density, which evokes associations with McConnell's rule⁵⁰ ($A_i = Q\rho_i$) for indirect proton hyperfine coupling in π -electron systems.⁵¹

We return finally to the unanswered question of associating the assigned A and B parameters with particular nitrogen atoms. Bersohn⁵² has calculated by simple molecular orbital theory the spin densities in hydrazyl and carbazyl. He finds for hydrazyl, densities of 0.1416 and 0.1518 on α and β , respectively; for carbazyl 0.1064 and 0.2061. The magnitudes of these densities are too small by a factor of at least two to account for the observed anisotropic coupling constants.⁵³ We suggest that extension of the calculation to include configuration interaction could possibly remove this disparity, for introduction of negative spin densities into some parts of the molecule would necessarily enhance the positive densities of other parts, very likely including the central nitrogens. Notwith-

⁵⁰ H. M. McConnell, *J. Chem. Phys.* **24**, 632, 764 (1956).

⁵¹ We have neglected the possibility that the degree of hybridization is the same in the four nitrogen atoms in question. Also, we do not intend to imply that the same proportionality extends to nitrogen atoms in other radicals.

⁵² R. Bersohn, *Arch. sci. (Geneva)* **11**, 177 (1958).

⁵³ If both these densities and the B constants were correct, the effective shielding parameters would necessarily have average values of 1.30 and 1.52 in hydrazyl and carbazyl, respectively. See footnote 38.

standing the omission of configuration interaction in the Bersohn calculation, it is quite probable that the *relative* densities on the α and β atoms are essentially correct. We would then have ρ_α/ρ_β equal to 0.93 in hydrazyl, 0.52 in carbazyl. The corresponding ratios B_2/B_1 are 0.88 and 0.53. These figures suggest that the larger constants should be associated with the β nitrogen in both hydrazyl and carbazyl.

Note added in proof. Chen, Sane, Walter, and Weil⁵⁴ have recently studied N^{15} -labeled hydrazyl and have concluded that the larger isotropic coupling constant belongs to the β (picryl) nitrogen. Using carefully deoxygenated solvents, they find: $A_\alpha = 7.63 \pm 0.20$ gauss, $A_\beta = 9.90 \pm 0.20$ gauss.

ACKNOWLEDGMENTS

The authors wish to thank their colleagues at the Applied Physics Laboratory for many fruitful discussions on several phases of this work. In particular, the collaboration of Martin L. Peller and Monica R. Nees on the chemical aspects of the work was indispensable. Mrs. Sylvia Ellsworth aided in some of the line-shape computations. Dr. John A. Weil of Argonne National Laboratory communicated to us his results on hydrazyl and contributed several valuable suggestions on our work.

⁵⁴ M. M. Chen, K. V. Sane, R. I. Walter, and J. A. Weil, *J. Phys. Chem.* (to be published).